

Advanced analysis of seismic data to validate critical assumptions

Willem de Beer ^{a,*}, Roy William ^b, Septian Prahastudhi ^b, Mohammed Braim ^c

^a ESG Solutions, Australia

^b ESG Solutions, Indonesia

^c ESG Solutions, Canada

Abstract

Passive mine seismic data are mainly used for hazard assessment in various forms. Although geophysical methods generally do not provide absolute numbers, locations of density or velocity contrasts, seismic source mechanisms and stress directions can be determined. Stress inversions, using seismic moment tensors, and passive seismic tomography can be used to reach conclusions about the state and fabric of the rock mass at a given time. Stress inversions are useful in describing the stress field distribution of the rock mass at a given time and place. Tomographic methods are useful for tracking the influence of mining on the surrounding rock. Tomographic methods also provide information in areas where there is no seismic activity but which are traversed by seismic radiation.

These techniques are applied to a block cave to test and expand geotechnical models and illustrate the evolution of stress distribution in the rock.

Keywords: *seismicity, tomography, stress inversion, time lapse, model validation*

1 Introduction

Seismic monitoring systems acquire real-time data in mines all around the world. These systems deliver multidimensional data sets predominantly used for short-term hazard assessment. However, a mine is a multi-decade undertaking. In the exploration, resource estimation and feasibility study phases, a substantial body of information is collected and collated into geological models. During the design phase, rock mass characterisation is key. A design and feasibility study (Brown 2007) involves the selection of a mining method, a detailed design of underground excavations (size, shape, support requirements), infrastructure location and design, impacts of mining (environmental and local communities) reports, risk assessments (rockbursts, major instabilities), rock fragmentation studies, production level design and surface subsidence information. The data used include geology, surface and groundwater geology, topography, environmental and geotechnical. There is significant lag between studies and mining, when the rock mass is accessed and the validity of any assumptions tested. Once established, geotechnical models are rarely modified, even if new information comes to hand.

Underground or surface mining perturbs the existing stress equilibrium (Gibowicz & Kijko 1994) and transfers stress to other locations which can experience sudden inelastic deformation (seismic events) or stress changes below the detectability limit of a monitoring system. The former can be used to learn more about the rock mass properties at the location of the events, while the latter response could be detected by tomographic methods.

Seismicity from two block caves in one orebody at different elevations was studied in near real time for up-to-date information on local stress regimes and some rock properties (e.g. damage, failure plane

* Corresponding author. Email address: willem.debeer@esgsolutions.com

orientations). The mine was in a mountainous area, exploiting skarns hosted in sedimentary rocks and a limestone group. The sedimentary rocks are deformed by kilometre-scale folds containing sub-vertical reverse and thrust faults. Superimposed on this is a left-lateral strike-slip reactivation of reverse faults. The source of the mineralisation is intrusive complexes formed by I-type calc-alkalic magmas. The hanging wall mineralisation boundary is a skarn reaction front in sudden contact with barren marble. The geological environment is therefore characterised by strong stiffness contrasts between diorites, skarns and marble, and by several mine- and regional-scale faults intersecting the caves. The upper block cave was mature and almost fully exploited, resulting in a large mass of moving subsidence rock.

The creation of a large rubble-filled cave in block caving results in a commensurately large zone of influence hundreds or thousands of metres away from the cave. The examination of the stress, deformation and resultant change to rock structure beyond the immediate mining horizon presents opportunities to tactically adjust mining planning and geotechnical models before development reaches the relevant locations.

2 Methodology

2.1 Source mechanisms

Seismic events emit a radiation pattern that depends on the orientation of the source. There are three fundamental fracture types: shear, tensile opening and tensile closure. Composite and more complex failures are constructed from combinations of these. In the bulk rock mass, the seismic source mechanism is approximated by a set of equivalent forces which produce particle displacements or strains in the rock identical to those from the actual forces of the physical process at the source (Jost & Herrman 1989). Each pair of forces produces a moment and the ground displacement at a sensor is given by a convolution of a Green's function which represents the response of the rock mass to forces (elastic stress/strain response) and the seismic moment tensor (SMT). Close to excavations, the model may require modification as the excavations may form part of the source.

The particle displacements are combinations of strains inward towards and outward away from the source. The SMT can be solved for by matrix inversion to yield pressure-compressional (P) and tensile (T) strain axis directions, and a decomposition of the SMT. The SMT can be decomposed into a combination of: volume change, fracture opening and closing, also called the isometric component; shear, the double couple component; and the compensated linear vector dipole component, a hybrid mechanism. The solutions also determine two possible failure planes. The result of the SMT inversion can be summarised in a 'beachball' diagram which represents the inner lower focal hemisphere projection of the first motions at the source and the traces of the complementary failure planes.

In underground mining, pure slip events are less common than other source mechanisms around underground excavations. They are associated with planar structures such as faults and dykes, and occasionally movement along lithological contacts. They may occur at a distance from the excavations and may not be immediately directly related to the mining activity. Using multiple SMTs, a stress inversion can be performed to understand the stress field.

2.2 Stress inversion

Seismic stress inversion estimates the most likely local principal stress directions given the observed failure planes from seismic moment tensors. It also provides the shape ratio; an estimate of the relative difference between the principal stress magnitudes.

We implement the stress inversion using Vavryčuk (2014), based on one of the standard methods for determining a single-stress tensor that best fits a set of focal mechanisms (Michael 1984). The technique minimises the difference between the slip vector and the resolved shear stress vector on each fault plane. A Mohr–Coulomb failure criterion (Figure 1) is used to estimate the orientation of the principal stress direction which maximises the instability of the potential failure planes.

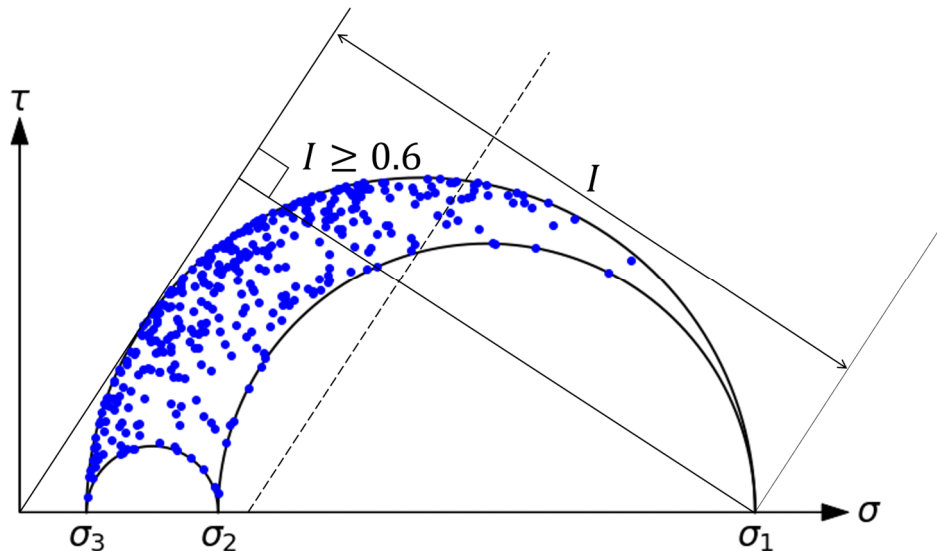


Figure 1 Mohr circle representing a single-stress tensor that best fits a set of focal mechanisms, with the individual inverted stress tensors for each event (blue dots). $I \geq 0.6$ indicates event/failure plane combinations most likely associated with failure

2.3 Passive seismic tomography

Rock fracturing generates seismic waves, which propagate with different velocities through parts of the rock mass with different moduli. Seismic tomography allows the reconstruction of changes in seismic velocities related to rock property variations by inverting the travel times of seismic waves. The variation of P-wave (V_p) and S-wave (V_s) velocity can help interpret lithology, stress and the state of deformation or damage.

V_p is a combination of bulk and shear modulus normalised by material density and V_s is shear modulus normalised by material density. Areas of increasing stress should show increasing velocities. Increasing stress translates to closing joints, fractures and microcracks along grain boundaries of rock, and to the increasing stiffness of the rock. Areas of decreasing velocities can be interpreted as destressing and/or post-peak rock failure. The sensitivity of body wave velocity to stress varies from approximately 0.1 to 1% change in velocity when stress changes (Niu et al. 2008; Silver et al. 2007; Yamamura 2003). A stress variation of 10 MPa would yield deviation from the background velocity ranging from 1 to 10%.

The volume of interest is discretised into a grid of 3D volume elements and the events are grouped by the volume in which they occur. Using the measured travel times of seismic signals from source-sensor pairs and a starting velocity model, a 1D background velocity (half space) is perturbed to generate a 3D velocity model. Initial inputs can consist of blasts and microseismic events (anything that can be located accurately). By examining the changes in velocity, cave shapes and stress changes can be estimated. The inversions used here utilised a modified form of the simultaneous iterative reconstruction technique (Tarantola & Valette 1982; Crowley et al. 2015).

2.4 Collapsing

The point locations calculated from a seismic system may obscure possible regular patterns in the spatial distribution of events. The collapsing method (Jones & Stewart 1997) enhances the spatial distribution of calculated seismic event locations by moving the location solutions inside their uncertainty ellipsoids until a distribution is obtained that is internally consistent. If event locations collapse to linear patterns, a linear geological structure could be inferred. This is a simple way to examine if a rock mass has any obvious dominant structures. If no clear structures are delineated, more subtle sources may be involved.

3 Data

3.1 Large block between two mine-scale faults

Figure 2 shows a large block of rock behind the slope of the upper cave (Cave 01) subsidence zone, bounded by northeast–southwest trending vertical mine-scale faults. Cave 01 is above and laterally offset from Cave 02. Seismicity was characterised by frequent large, slow and complex events in a soft rock environment, with no damage to mine infrastructure. The moment tensor solutions for the large events suggested an association with the geological structures and was speculated to be related to large blocks of rock moving vertically along the faults, which will be depicted in the next section.

Historical exploration drilling data did not indicate additional large geological structures between the regional-scale structures. The locations of 8,132 events were collapsed in Figure 3, with inconclusive results (low data quality, $DQ \leq 0.5$ and high location error, $LE \geq 50$ m). With well-constrained sensor coverage, the theoretical location accuracy in the area of interest is between 10–25 m. In this period, over 80 sensors (a combination of 15 Hz and 4.5 Hz geophones) were installed in both mines as well as several broadband seismometers at distances ranging from several to hundreds of kilometres from the mines.

Data were collected by recording the ground motion continuously at a sampling frequency of 5,000 Hz. The system uses an automatic trigger capture feature based on a dynamic voltage threshold exceeded at a given sensor (usually the closest to the source of the perturbation). Waveforms from all the sensors in the system are then captured in a trigger. An automatic processing algorithm then picks possible arrival times and classifies the trigger as a valid seismic event, blasting or noise, and calculates the source parameters.

A stress inversion was performed using 223 moment tensor solutions which exhibited varying mechanisms and failure types (Figure 4) but which did show discernible trends in the P and T axes. Stress inversion indicated that there was a propensity for the rock mass to fail in preferred directions.

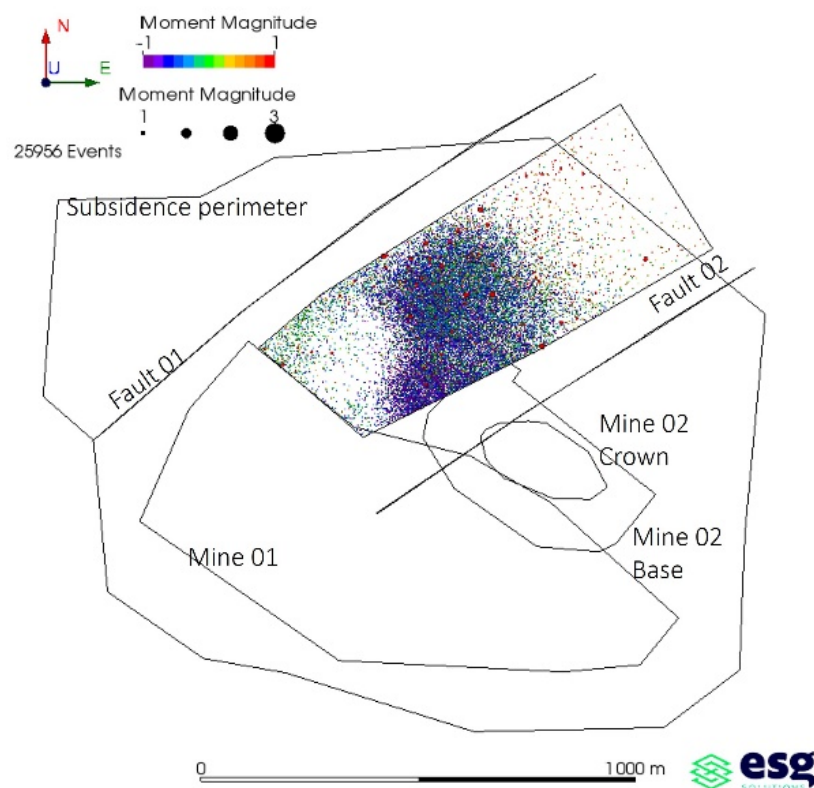


Figure 2 Seismicity in a block between two mine-scale faults over an 11-month period. Events are coloured by moment magnitude

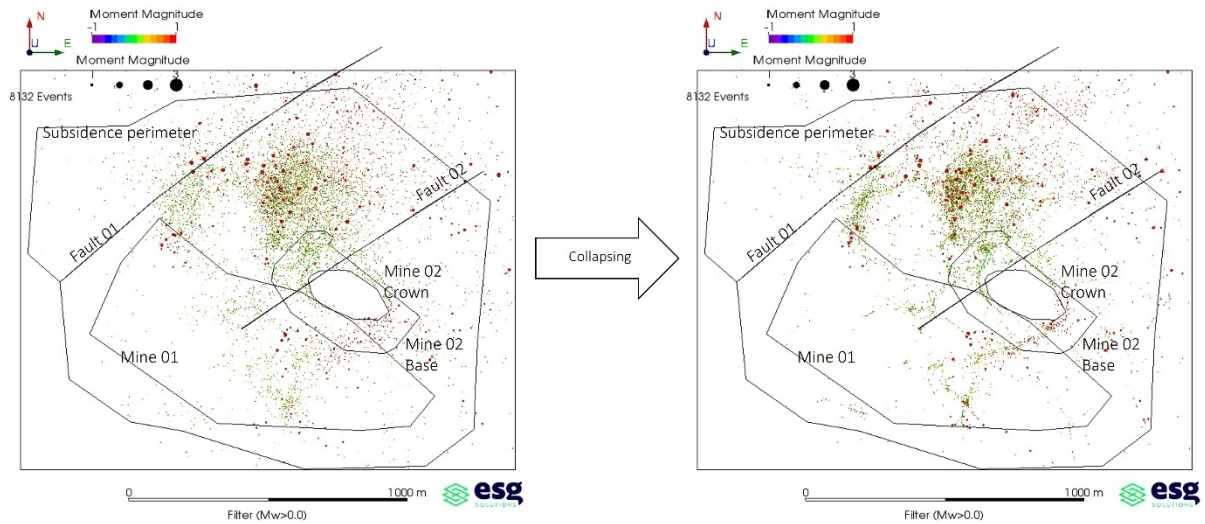


Figure 3 Collapsing event clouds in this case are not yielding any obvious linear features

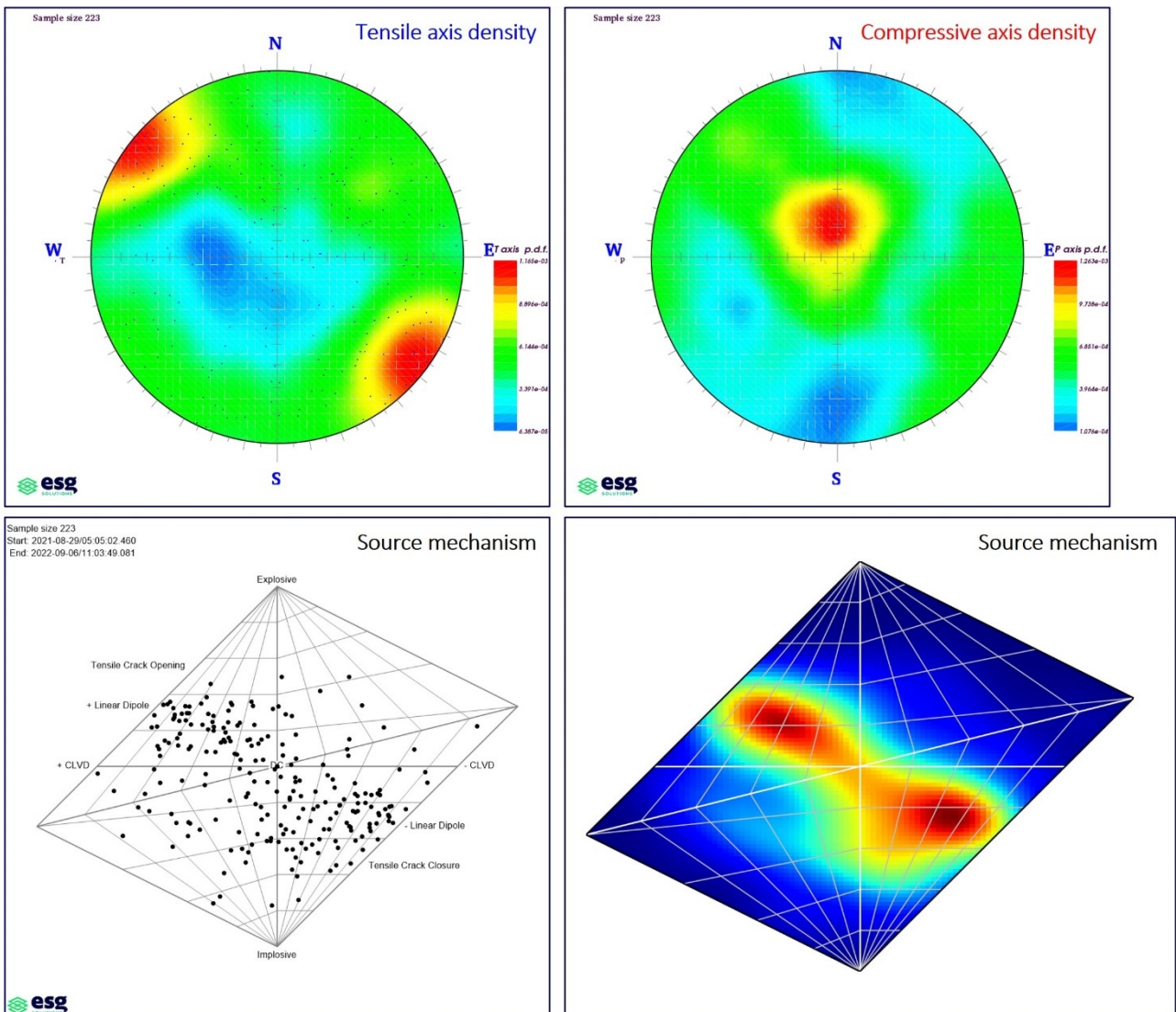


Figure 4 Clockwise from top left: tensile (T) strain axis density; compressive (P) axis density; Hudson (Hudson et al. 1989) source type diagram

3.2 Cave abutment

The modification of the local stress field around an excavation grows with the size of the excavation (Brady & Brown 2004). Seismic events occurring in the abutments of an excavation are the result of this modification. Abutment seismicity therefore presents an opportunity to learn more of both the effect of the excavation and the rock mass itself.

3.2.1 Stress inversions

A region to the northwest of the developing Cave 02 became seismically active and remained so for several years (Figure 5). The seismicity was located in a region between the same faults discussed previously, but approximately 400 m deeper. To gain an impression of the change in stress as the cavefront approached, two overlapping time periods were considered. Overlapping was needed to have enough moment tensor solutions for stable stress inversions. The collapse analysis of the solutions in the two overlapping time periods showed no linear patterns. In time span 01, 158 events had high-confidence moment tensor solutions. Time span 02 had 183 events with high-confidence moment tensor solutions. High confidence requires that the correlation coefficient of a linear fit of sensor theoretical displacement spectrum plateaus to recorded plateaus, $r^2 \geq 0.7$, and that the condition number, CN, a measure of the stability of the solution based on array coverage, is ≤ 35 . The mechanisms and failure types varied (Figure 6) but trends in the P and T axes were evident. Stress inversion indicated that there was a propensity for the rock mass to fail in preferred directions.

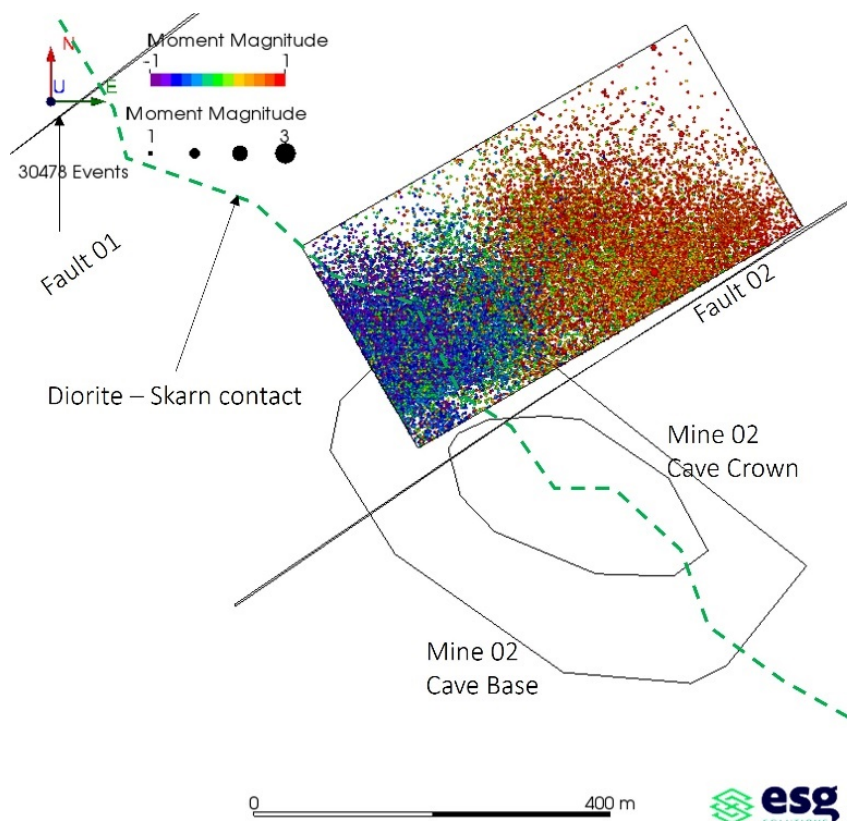


Figure 5 Seismicity in the cave abutment. Events are coloured by moment magnitude

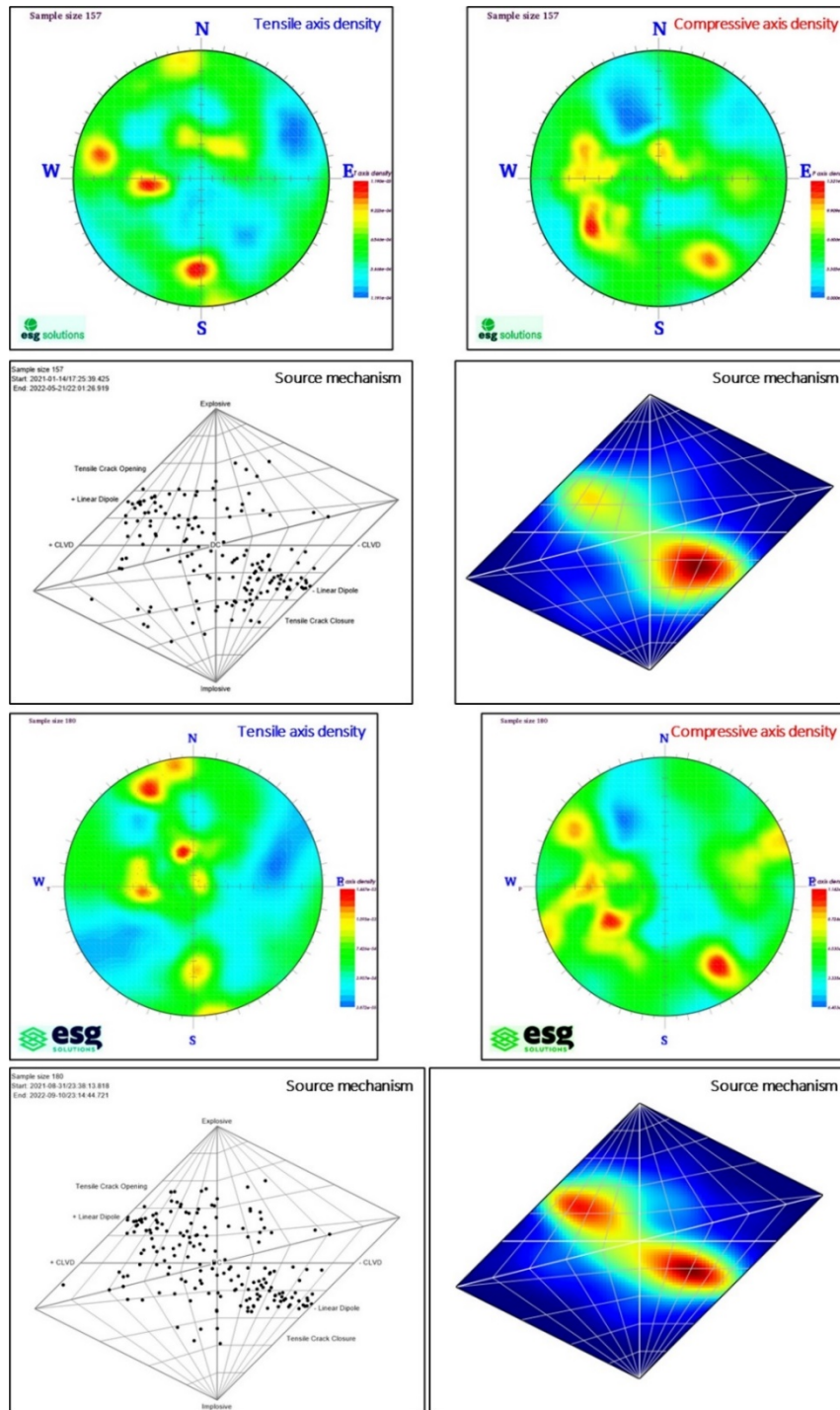


Figure 6 Clockwise from top left: tensile (T) strain axis density; compressive (P) axis density; Hudson (Hudson et al. 1989) source type diagram; Time span 01, in cave abutment Bottom: same for Time span 02

3.2.2 Passive seismic tomography

Time-lapse passive seismic tomography was performed for Mine 02 in one-month windows to examine the evolution of the abutment. Figure 7 compares the results to known large-scale lithology. In both time frames the tomography captures the difference between diorite and skarn at the base of the cave very well. This is to be expected from large, mostly unchanging geological features. P- and S-wave velocities in skarn are higher than in diorite as the density and Poisson's ratio values are higher than in diorite. This is supported by velocity calibrations using blasts.

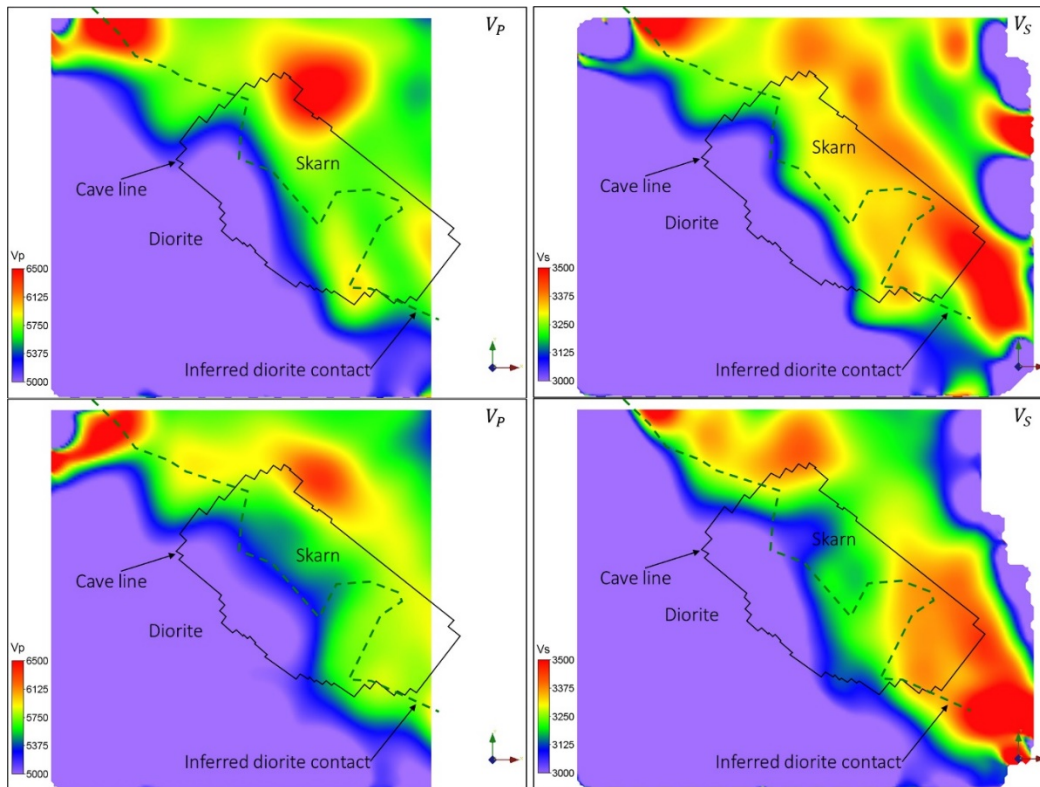


Figure 7 Contours of inverted P-wave velocity (left) and S-wave velocity (right) on a cut plane through the extraction level of Mine 02, Month 01 (top) and Month 02 (bottom). The contrast between low and high inferred velocities roughly follows the contact between stiff and brittle diorite and the skarn

4 Results

4.1 Stress inversions

In the first case study there was substantial seismic activity in a block between mine-scale faults, but the geological database did not have any structures which could be considered sources for the activity. Collapsing event locations (Figure 3) did not conclusively highlight linear structures, while source mechanisms (Figure 4) were variable, with some indication of dominant opening and closing type mechanisms. Stress inversion results (Figure 8) suggested a steeply dipping to sub-vertical σ_1 (Table 1). The σ_1 direction was consistent with stress measurements (GA 2018) for depth <900 m. The effective failure plane dips steeply (Figure 8). In Figure 8 the results are summarised graphically. The failure plane is shown as a single plane but the interpretation is that, on average, the sense of dislocation is steeply dipping. In other words, many shallow dipping fractures were opening and closing. The hypothesis was that subsidence and downward block movement between the faults were driving bedding plane and/or joint sliding, opening or closing. In other words, there was a lot of collective movement presenting as slow, large-deformation seismic events rather than slip on faults.

Stress inversion results for the abutment of Cave 02 (Figure 9), the cave below the large block discussed above, suggested a shallow dipping to sub-horizontal σ_1 (Table 1). The σ_1 direction was consistent with stress measurements (GA 2018) for depth >900 m, roughly consistent with the accepted ambient tectonic stress. The average effective failure plane was steeply dipping (Figures 9 and 10) and the source mechanisms were diverse, with some preponderance of opening and closing.

The subsidence and associated rebound (Cave 01) could have been unclamping pre-existing shear zones. At this depth the stress conditions were still close to the background tectonic situation, but there was some suggestion of local stress rotation by the approaching cave.

Table 1 Principal stress and failure plane solutions

Item	Trend	Plunge
Large block between mine-scale faults		
σ_1	260	76°
σ_2	45°	10°
σ_3	136°	7°
Failure plane	25°	64°
Cave abutment – time span 01		
σ_1	237°	11°
σ_2	61°	62°
σ_3	332°	24°
Failure plane	14°	60°
Cave abutment – time span 02		
σ_1	240°	5°
σ_2	140°	40°
σ_3	337°	49°
Failure plane	17°	71°

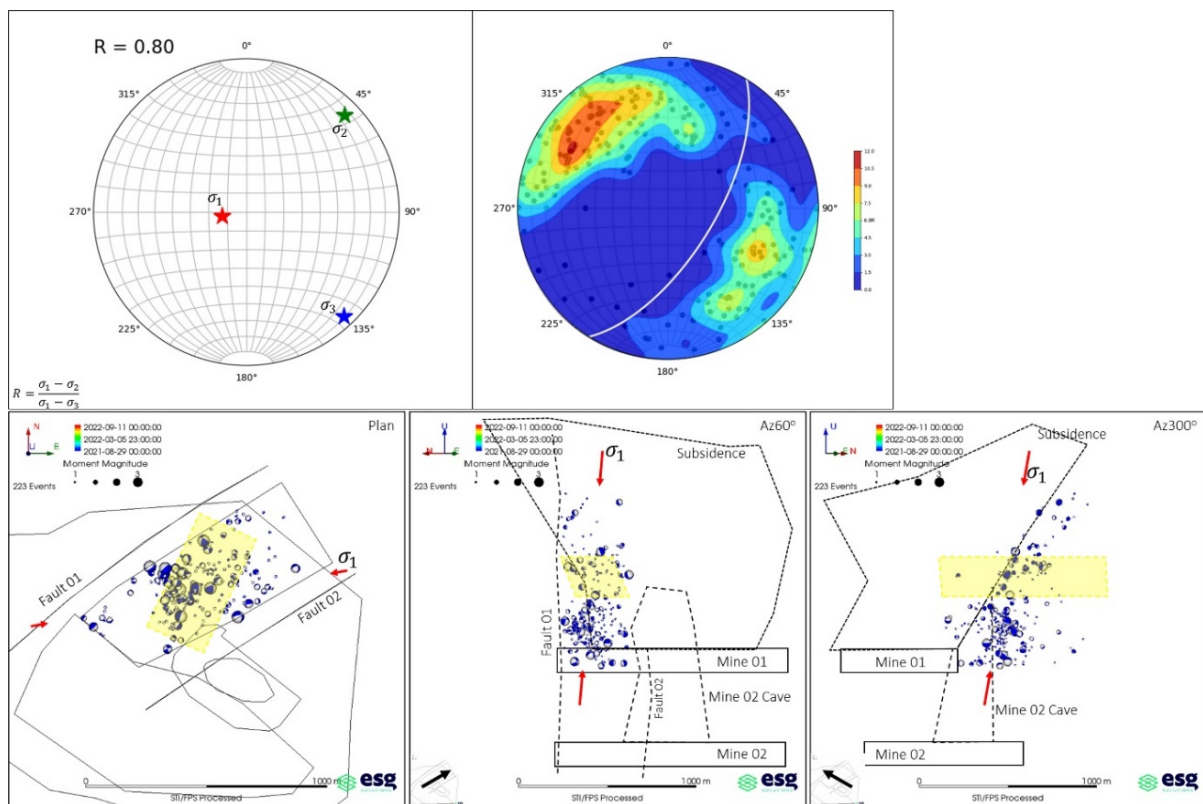


Figure 8 Top: Stable solutions for the principal stress directions, shape factor and average effective failure plane (yellow square) in a large block between two mine-scale faults. Bottom: Interpreted σ_1 and failure plane in a large block between two mine-scale faults

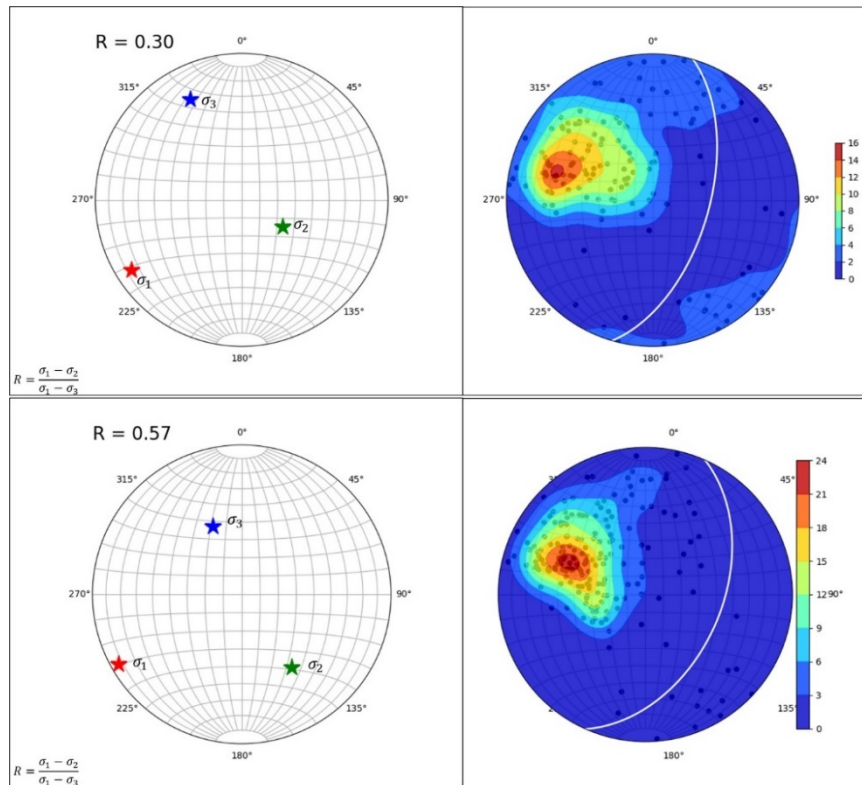


Figure 9 Stable solutions for the principal stress directions and shape factor in the abutment of a cave, Time span O1 (top) and Time span O2 (bottom)

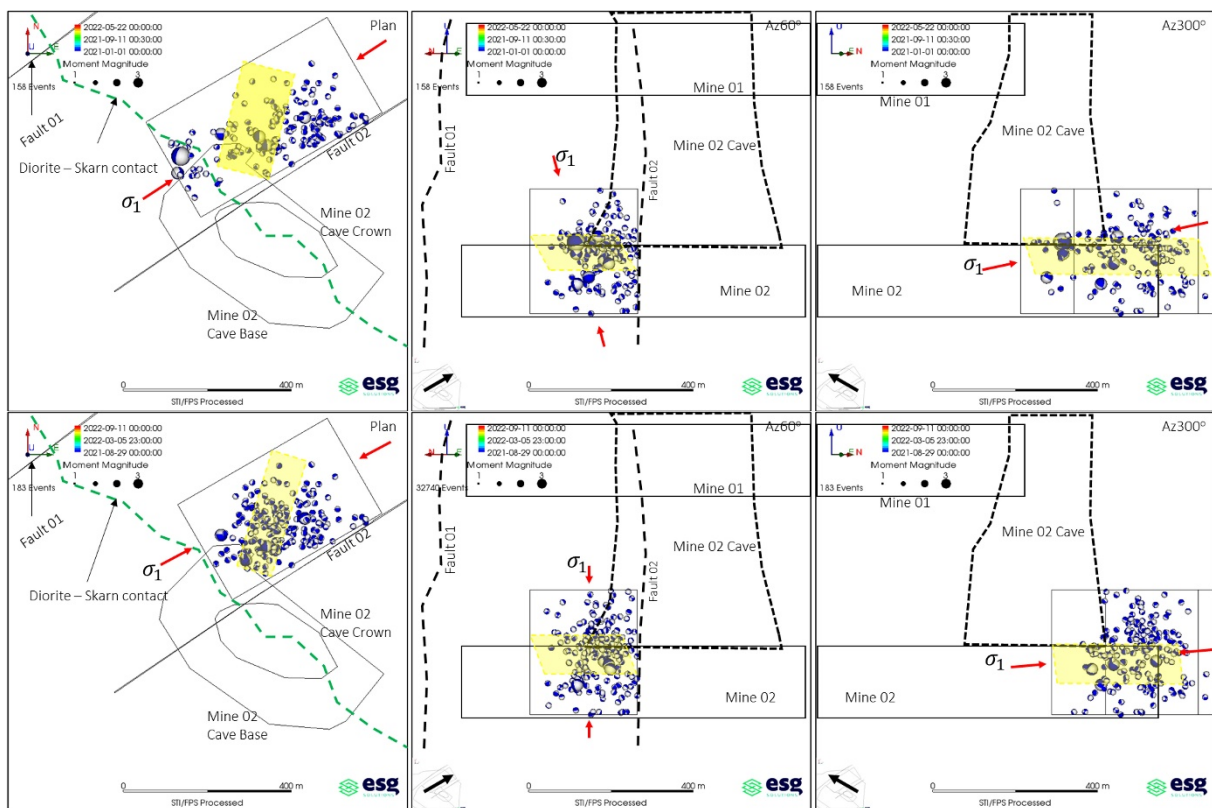


Figure 10 Interpreted σ_1 and failure plane (yellow rectangle) in the abutment of a cave: Time span O1 (top) and Time span O2 (bottom)

4.2 Passive tomography

In contrast to the lithological contact in Mine O2 (Figure 7), substantial differences between the two months in the tomographic inversions were evident in the abutment (Figure 11). These time periods were both in time span O2 of the stress inversion exercise.

It is important to remember that the presumed cave outline is an abstraction derived from open hole measurements, height of draw calculations and seismic location distributions. There is a lag between measurements and updates, so the presumed outline is always out of date. The cave outline drawing has a sharp boundary between the cave and the host rock but the transition is more gradual. The inversion grid size is 50 m, which limits the resolution of the method. These factors could partly explain why the tomography results in Figure 11 do not reproduce exactly the abstracted cave outline. Nevertheless, the inversion does capture the general location of the cave.

Comparing the P-wave velocity results in months O1 and O2 and using the P-wave velocity as a proxy for stress, it appears that a larger fraction of the abutments experienced higher stress than the background in month O1. In month O2 the higher stress volume was more concentrated and appeared to extend upwards more. The S-wave velocity, which is sensitive to fracture density and orientation, supports this interpretation. It appears as if the further abutment has yielded in the two months, and the higher stresses closer to the assumed cave front are driven by production activity (blasting and mucking). In general the velocity values are lower, indicating lower stress or yielded areas.

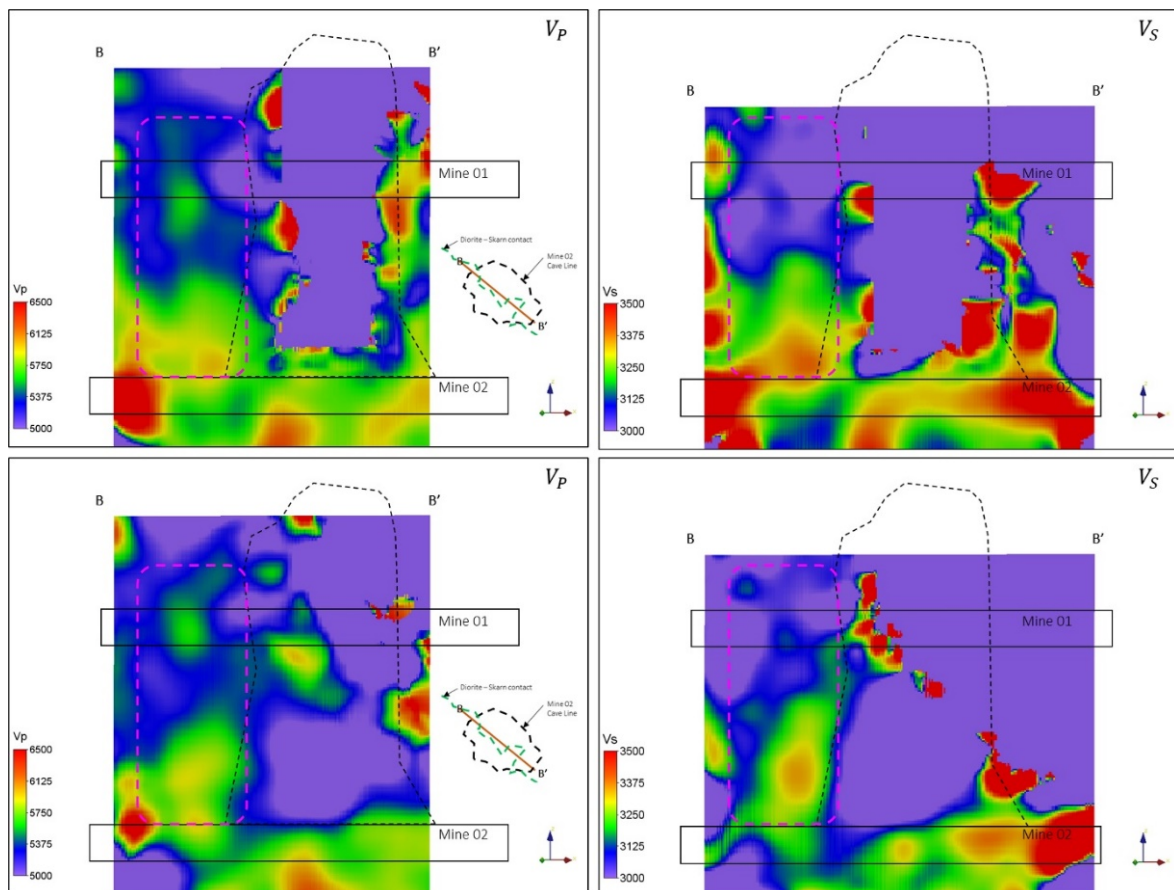


Figure 11 Contours of inverted P-wave velocity (left) and S-wave velocity (right) in the northwestern abutment of the Mine O2 cave: Month O1 (top); Month O2 (bottom). Cut plane through the centreline of the presumed cave (dotted line). The area of interest is indicated by the dashed magenta oblong

5 Conclusion

The main current use of mine seismic monitoring systems is short-term hazard assessment and risk management. However, if a system can deliver data which can be used for stress inversions and passive tomography, the possibility exists to use the system as a strategic tool. Computing power and algorithms exist to perform clustering, moment tensor inversion, stress inversion and tomographic inversions in near real time.

The data used must conform to strict conditions. Tomographic inversions require a high degree of uniformity in the spatial distribution of events. Stress inversions require moment tensors which in turn require accurate source locations, and at least seven fully operational triaxial sensors in the far field of the source, arranged in a wide (if not fully 3D) angular coverage of the focal sphere. P- and S-wave first motions at sensors (including polarisation) must be determined accurately, as must the spectral amplitude measurement from P- and S-waves. This means that seismic monitoring arrays must be carefully designed with a mix of sensors, and that installation must be done with care and attention to detail. Ongoing preventive maintenance and uncompromising quality control are essential.

Various ways of clustering data, including the collapsing technique shown here, combined with stress inversions to estimate the most likely failure planes (or collections of planes) could provide indications of the rock mass structure ahead of mining. Small faults and dykes are frequently missed during exploration drilling, and topography and other environmental conditions can preclude on-the-ground geophysical techniques. When mine-scale faults and dykes are detected their extent and persistence is mostly a matter of judgement. The expanding stress perturbation and deformation around an excavation activate structures or bedding planes and shear zones. If these activated structures are significant dykes or faults they must be approached carefully.

Local in situ stress is a significant variable which is very hard to determine directly. The world stress map (Heidbach et al. 2016) does not have the required resolution and is based on tectonic earthquakes at depths far exceeding the deepest mine. The upper 1,000 to 3,000 m of the crust is heterogeneous and disordered, and topography can affect local stress conditions. This is important as the local stress magnitude and direction affect the response of excavations. A large enough excavation can change local principal stress directions. It is therefore important and useful to have a technique that can be applied in near real time to track local stress evolution.

While stress inversion cannot provide absolute values for the stress, the shape factor carries some indication of relative magnitudes. Passive seismic tomography can highlight areas of higher stress than others and can show how the stress changes. Rock mass changes can be observed from the damage or displacement that occurred in the abutment area or around mine infrastructure that is connected to the affected local structures. This damage is likely to occur in areas that have experienced high stress previously or are identified by seismically active zones. An important use of this information is to judge when the stress perturbation ahead of cave development has migrated. This can assist in sequencing mining from low to high stress as well as deciding where to deploy resources to increase the production rate in distressed areas while higher stress areas pass through a stress peak.

Practical use of the results requires some thought and discussion. In most mining scenarios, changing mine layouts rapidly is unfeasible. These changes always mean loss of production and may require retooling, training and additional people. However, there is considerable room for variation in support strategies, sequencing and the rate of mining which could result in small but important improvements in geometry or stress migration.

Acknowledgement

The authors wish to thank Samantha Palmer (ESG Solutions Canada) for the detailed internal review and suggestions.

References

- Brady, BHG & Brown, ET 2004, *Rock Mechanics for Underground Mining*, Springer, Berlin, pp. 197–223.
- Brown, ET 2007, *Block Caving Geomechanics 2nd Ed. – the International Caving Study 1997–2004*, Julius Kruttschnitt Mineral Research Centre, The University of Queensland, St Lucia.
- Crowley, JW, Baig, AM, Urbancic, T & Von Lunen, E 2015, '4D tomography and deformation from microseismic data', *Proceedings of the 77th EAGE Conference and Exhibition*.
- GA 2018, Confidential consultant's report.
- Gibowicz, SJ & Kijko, A 1994, *An Introduction to Mining Seismology*, Academic Press, Cambridge.
- Heidbach, O, Rajabi, M, Reiter, K, Ziegler, M & WSM Team 2016, *World Stress Map Database Release 2016. V. 1.1*, GFZ Data Services. <https://doi.org/10.5880/WSM.2016.001>
- Hudson, J, Pearce, R & Rogers, R 1989, 'Source type plot for inversion of the moment tensor', *Journal of Geophysical Research: Solid Earth*, vol. 94, pp. 765–774.
- Jones, R & Stewart, R 1997, 'A method for determining significant structures in a cloud of earthquakes', *Journal of Geophysical Research: Solid Earth*, vol. 102, pp. 8245–8254.
- Jost, ML & Herrmann, RB 1989, 'A student's guide to and review of moment tensors', *Seismological Research Letters*, vol. 60, pp. 37–57.
- Michael, AJ 1984, 'Determination of stress from slip data: faults and folds', *Journal of Geophysical Research: Solid Earth*, vol. 89, pp. 11517–11526.
- Niu, F, Silver, PG, Daley, TM, Cheng, X & Majer, EL 2008, 'Preseismic velocity changes observed from active source monitoring at the Parkfield SAFOD drill site', *Nature*, vol. 454, pp. 204–208.
- Silver, PG, Daley, TM, Niu, F & Majer, EL 2007, 'Active source monitoring of cross-well seismic travel time for stress-induced changes', *Bulletin of the Seismological Society of America*, vol. 97, pp. 281–293, <https://doi.org/10.1785/0120060120>
- Tarantola, A & Valette, B 1982, 'Generalised nonlinear inverse problems solved using the least squares criterion', *Reviews of Geophysics*, vol. 20, no. 2, pp. 219–232.
- Vavryčuk, V 2014, 'Iterative joint inversion for stress and fault orientations from focal mechanisms', *Geophysical Journal International*, vol. 199, pp. 69–77.
- Yamamura, K 2003, 'Long-term observation of in situ seismic velocity and attenuation', *Journal of Geophysical Research*, vol. 108, <https://doi.org/10.1029/2002JB002005>

